Nanostructured intermetallic InSb as a new high capacity and high-performance negative electrode for sodium-ion batteries

Irshad Mohammad[*†], *Lucie Blondeau*[†], *Eddy Foy*[§], *Jocelyne Leroy*[‡], *Eric Leroy*[⊥], *Hicham Khodja*[†], *Magali Gauthier*[*†]

[†] Université Paris-Saclay, CEA, CNRS, NIMBE, LEEL, 91191, Gif-sur-Yvette, France

[§] Université Paris-Saclay, CEA, CNRS, NIMBE, LAPA-IRAMAT, 91191 Gif-sur-Yvette, France

[‡] Université Paris-Saclay, CEA, CNRS, NIMBE, LICSEN, 91191 Gif-sur-Yvette, France

[⊥] Université Paris Est Créteil, CNRS, ICMPE, UMR 7182, 2 rue Henri Dunant, 94320 Thiais, France

* Corresponding authors: irshad.mohammad@cea.fr; magali.gauthier@cea.fr

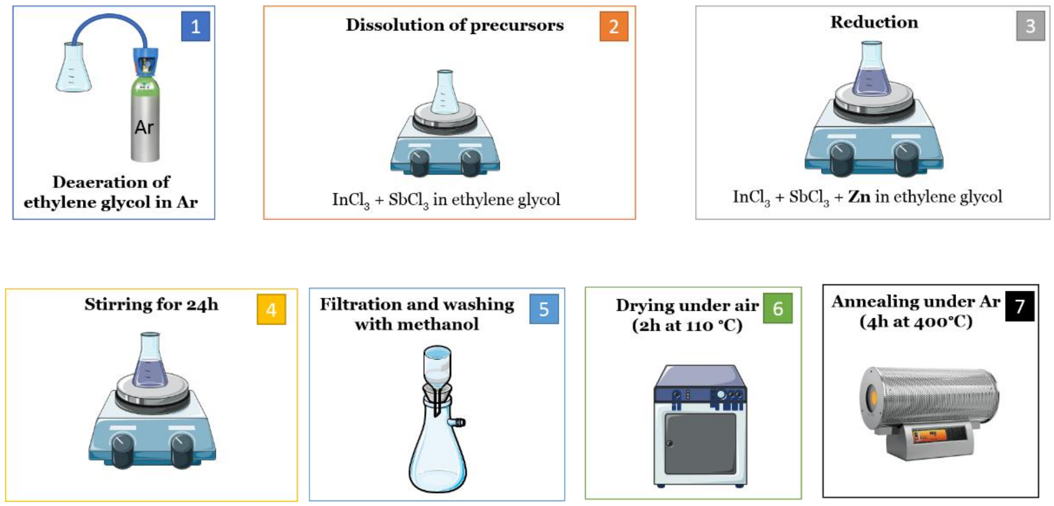

Figure S1. Schematic description of the reduction synthesis process for the InSb or Sb powders.

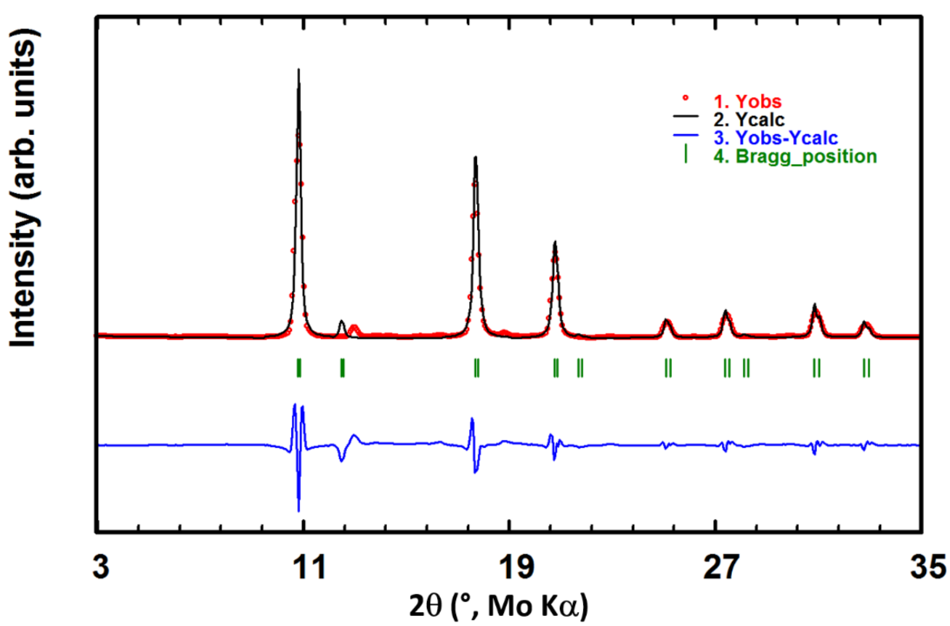

Figure S2. Observed and calculated XRD patterns of as-prepared InSb.

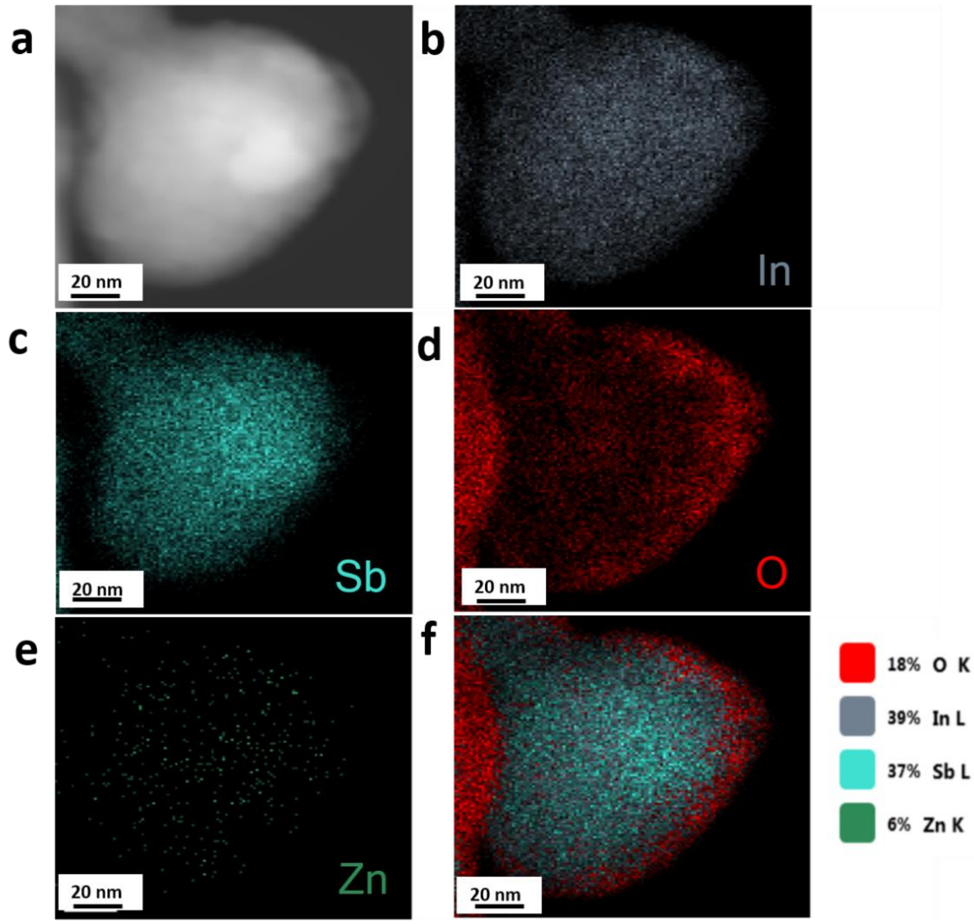

Figure S3. EDX images of the nanostructured InSb powder. (a) electron image and (b-f) the corresponding elemental mapping images of O, In, Sb and Zn. The corresponding atomic percentages of elements are given in (f).

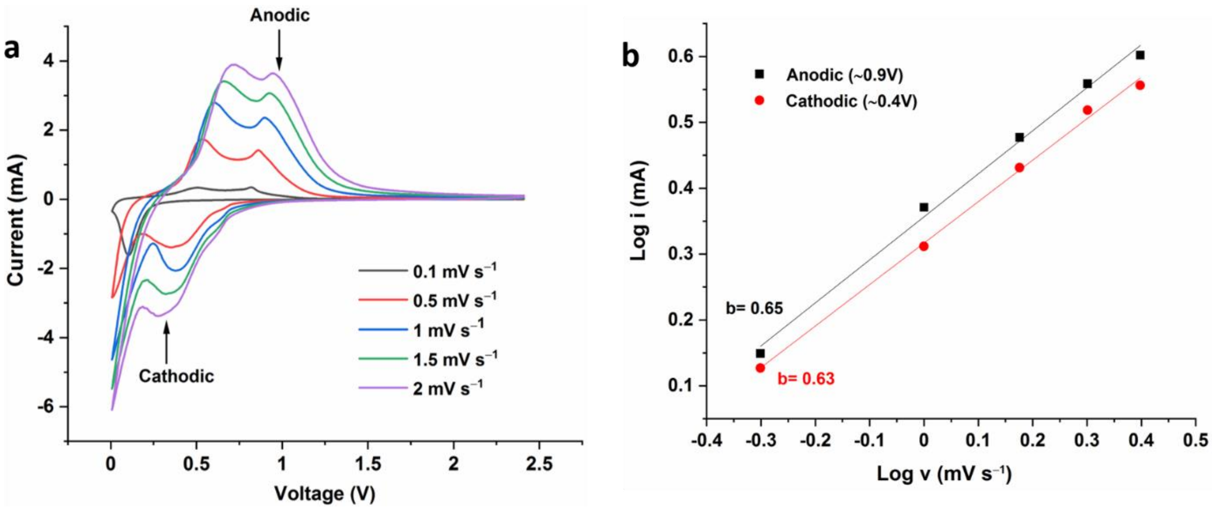

Figure S4. (a) CV curves of the InSb electrode upon reaction with sodium at different scan rates. (b) Relationship of the InSb anodic and cathodic peaks against the scan rate to determine *b* values.

Table S1. Comparison of the performance of alloy-based materials with the performance of nanostructured InSb obtained in this study.

Anode Materials	**1st charge capacity (mAh g–1)**	**Current Density (mA g–1)**	**Cycle life (mAh g–1)**	**Synthesis method**	**Ref.**
Crystalline Sb	537	0.5C	576 (80th)	Ball milling	[1]
Sb-C	559	0.1C	430 (195th)	Chemical route	[2]
Sb–C nanofibers	632	40	446 (400th)	Electrospinning	[3]
Sb/N-C nanosheets	340	50	305 (60th)	Sol–gel route	[4]
Sb hollow nanospheres	645	50	622 (50th)	Galvanic replacement	[5]
AlSb film	450	0.16C	250 (50th)	Magnetron sputtering	[6]
SnSb/C nanocomposite	544	100	435 (80th)	High energy ball milling	[7]
Sb_2O_3	331	500	414 (200th)	Electro Spray Deposition	[8]
Sb_2S_3-graphite	662	1000	665 (100th)	High energy ball milling	[9]
Nanoporous Bi-Sb	551	200	257 (200th)	Chemical dealloying	[10]
Sb_2S_5	845	100	774 (300th)	Hydrothermal method	[11]
Sb-Si	585	200	663 (140th)	Cosputtering	[12]
Sn-Ge-Sb	833	85	662 (50th)	Cosputtering	[13]
Mo_3Sb_7	400	0.2C	338 (800th) at 0.5C	Solid-state synthesis	[14]
Ni-Sb	632	60	500 (70th)	Chemical synthesis	[15]
FeSb-TiC-C nanocomposite	215	100	210 (60th)	High energy ball milling	[16]
3D porous Sb-Co composite	718	60	578 (50th)	Reduction precipitation	[17]
β-SnSb film	700	200	470 (150th)	Sputtering	[18]
Zn_4Sb_3 thin films	474	0.2C	394 (100th)	Electrodepostion	[19]
Nanostructured Sb_2Te_3–C	410	50	373 (50th)	Solid-state synthesis	[20]
Sb@Co(OH)$_2$ nanosheet	973	200	749 (200th)	Magnetron sputtering	[21]
Sn(10)-Bi(10)-Sb(80)	621	200	614 (100th)	Sputtering	[22]
In–Sb–S framework	543	50	330 (50th)	Surfactant-thermal strategy	[23]
InSb	287	50	400 (250th)	Mechanical alloying	[24]
Nanostructured InSb	440 361	0.2C (110) C (570)	450 (50th) 360 (100th)	Chemical reduction	*This work

Table S2. Theoretical volume expansion (ΔV) of binary Na–M compounds calculated by Vegard's law [25]. The molar volume occupies by Na in the Na–M alloys is V=18.2 mL mol^{-1} [26].

Element	**Density (g·cm^{-3})**	**$V_{Element}$ [mL.mol^{-1}]**	**Reduction Product**	**$V_{Reduction\ Product}$ [mL.mol^{-1}]**	**ΔV [%]**
Si	2.33	12.05	NaSi	30.25	~ 150
Ge	5.32	13.65	NaGe	31.85	~ 130
Sn	7.29	16.28	$Na_{15}Sn_4$	84.53	~ 420
Pb	11.35	18.25	$Na_{15}Pb_4$	72.85	~ 300
P (Black)	2.34	13.17	Na_3P	67.83	~ 410
Sb	6.70	18.17	Na_3Sb	72.51	~ 300
In	8.31	15.70	NaIn	33.90	~ 115
Bi	7.31	21.36	Na_3Bi	75.96	~ 250
As	5.72	13.08	Na_3As	67.68	~ 420

References

[1] A. Darwiche, C. Marino, M. T. Sougrati, B. Fraisse, L. Stievano, and L. Monconduit, "Better Cycling Performances of Bulk Sb in Na-Ion Batteries Compared to Li-Ion Systems: An Unexpected Electrochemical Mechanism," *J. Am. Chem. Soc.*, vol. 134, no. 51, pp. 20805–20811, Dec. 2012, doi: 10.1021/ja310347x.

[2] X.-M. Pham *et al.*, "A self-encapsulated porous Sb–C nanocomposite anode with excellent Na-ion storage performance," *Nanoscale*, vol. 10, no. 41, pp. 19399–19408, Oct. 2018, doi: 10.1039/C8NR06182C.

[3] L. Wu *et al.*, "Sb–C nanofibers with long cycle life as an anode material for high-performance sodium-ion batteries," *Energy Environ. Sci.*, vol. 7, no. 1, pp. 323–328, Dec. 2013, doi: 10.1039/C3EE42944J.

[4] X. Zhou, Y. Zhong, M. Yang, M. Hu, J. Wei, and Z. Zhou, "Sb nanoparticles decorated N-rich carbon nanosheets as anode materials for sodium ion batteries with superior rate capability and long cycling stability," *Chem. Commun.*, vol. 50, no. 85, pp. 12888–12891, Sep. 2014, doi: 10.1039/C4CC05989A.

[5] S. Qiu, X. Wu, L. Xiao, X. Ai, H. Yang, and Y. Cao, "Antimony Nanocrystals Encapsulated in Carbon Microspheres Synthesized by a Facile Self-Catalyzing Solvothermal Method for High-Performance Sodium-Ion Battery Anodes," *ACS Appl. Mater. Interfaces*, vol. 8, no. 2, pp. 1337–1343, Jan. 2016, doi: 10.1021/acsami.5b10182.

[6] L. Baggetto, M. Marszewski, J. Górka, M. Jaroniec, and G. M. Veith, "AlSb thin films as negative electrodes for Li-ion and Na-ion batteries," *Journal of Power Sources*, vol. 243, pp. 699–705, Dec. 2013, doi: 10.1016/j.jpowsour.2013.06.074.
[7] Y. Zhao and A. Manthiram, "High-Capacity, High-Rate Bi–Sb Alloy Anodes for Lithium-Ion and Sodium-Ion Batteries," *Chem. Mater.*, vol. 27, no. 8, pp. 3096–3101, Apr. 2015, doi: 10.1021/acs.chemmater.5b00616.
[8] M. Hu, Y. Jiang, W. Sun, H. Wang, C. Jin, and M. Yan, "Reversible conversion-alloying of Sb2O3 as a high-capacity, high-rate, and durable anode for sodium ion batteries," *ACS Appl Mater Interfaces*, vol. 6, no. 21, pp. 19449–19455, Nov. 2014, doi: 10.1021/am505505m.
[9] Y. Zhao and A. Manthiram, "Amorphous Sb2S3 embedded in graphite: a high-rate, long-life anode material for sodium-ion batteries," *Chem. Commun.*, vol. 51, no. 67, pp. 13205–13208, Aug. 2015, doi: 10.1039/C5CC03825A.
[10] H. Gao, J. Niu, C. Zhang, Z. Peng, and Z. Zhang, "A Dealloying Synthetic Strategy for Nanoporous Bismuth–Antimony Anodes for Sodium Ion Batteries," *ACS Nano*, vol. 12, no. 4, pp. 3568–3577, Apr. 2018, doi: 10.1021/acsnano.8b00643.
[11] Y. Lu *et al.*, "High-Capacity and Ultrafast Na-Ion Storage of a Self-Supported 3D Porous Antimony Persulfide–Graphene Foam Architecture," *Nano Lett.*, vol. 17, no. 6, pp. 3668–3674, Jun. 2017, doi: 10.1021/acs.nanolett.7b00889.
[12] W. P. Kalisvaart, B. C. Olsen, E. J. Luber, and J. M. Buriak, "Sb–Si Alloys and Multilayers for Sodium-Ion Battery Anodes," *ACS Appl. Energy Mater.*, vol. 2, no. 3, pp. 2205–2213, Mar. 2019, doi: 10.1021/acsaem.8b02231.
[13] B. Farbod *et al.*, "Anodes for Sodium Ion Batteries Based on Tin–Germanium–Antimony Alloys," *ACS Nano*, vol. 8, no. 5, pp. 4415–4429, May 2014, doi: 10.1021/nn4063598.
[14] W. Li *et al.*, "Carbon-coated Mo3Sb7 composite as anode material for sodium ion batteries with long cycle life," *Journal of Power Sources*, vol. 307, pp. 173–180, Mar. 2016, doi: 10.1016/j.jpowsour.2015.12.121.
[15] J. Liu, Z. Yang, J. Wang, L. Gu, J. Maier, and Y. Yu, "Three-dimensionally interconnected nickel–antimony intermetallic hollow nanospheres as anode material for high-rate sodium-ion batteries," *Nano Energy*, vol. 16, pp. 389–398, Sep. 2015, doi: 10.1016/j.nanoen.2015.07.020.
[16] I. T. Kim, E. Allcorn, and A. Manthiram, "High-performance FeSb–TiC–C nanocomposite anodes for sodium-ion batteries," *Phys. Chem. Chem. Phys.*, vol. 16, no. 25, pp. 12884–12889, Jun. 2014, doi: 10.1039/C4CP01240B.
[17] Y. Zhang *et al.*, "3D porous Sb-Co nanocomposites as advanced anodes for sodium-ion batteries and potassium-ion batteries," *Applied Surface Science*, vol. 499, p. 143907, Jan. 2020, doi: 10.1016/j.apsusc.2019.143907.
[18] H. Xie *et al.*, "β-SnSb for Sodium Ion Battery Anodes: Phase Transformations Responsible for Enhanced Cycling Stability Revealed by In Situ TEM," *ACS Energy Lett.*, vol. 3, no. 7, pp. 1670–1676, Jul. 2018, doi: 10.1021/acsenergylett.8b00762.
[19] E. D. Jackson, S. Green, and A. L. Prieto, "Electrochemical Performance of Electrodeposited Zn4Sb3 Films for Sodium-Ion Secondary Battery Anodes," *ACS Appl. Mater. Interfaces*, vol. 7, no. 14, pp. 7447–7450, Apr. 2015, doi: 10.1021/am507436u.
[20] K.-H. Nam, J.-H. Choi, and C.-M. Park, "Highly Reversible Na-Ion Reaction in Nanostructured Sb2Te3-C Composites as Na-Ion Battery Anodes," *J. Electrochem. Soc.*, vol. 164, no. 9, p. A2056, Jul. 2017, doi: 10.1149/2.1161709jes.

[21] "Scalable Fabrication of Core–Shell Sb@Co(OH)2 Nanosheet Anodes for Advanced Sodium-Ion Batteries via Magnetron Sputtering | ACS Nano." https://pubs.acs.org/doi/abs/10.1021/acsnano.8b07227 (accessed Jan. 04, 2021).

[22] H. Xie, W. P. Kalisvaart, B. C. Olsen, E. J. Luber, D. Mitlin, and J. M. Buriak, "Sn–Bi–Sb alloys as anode materials for sodium ion batteries," *J. Mater. Chem. A*, vol. 5, no. 20, pp. 9661–9670, May 2017, doi: 10.1039/C7TA01443K.

[23] L. Nie *et al.*, "Crystalline In–Sb–S framework for highly-performed lithium/sodium storage," *J. Mater. Chem. A*, vol. 5, no. 27, pp. 14198–14205, Jul. 2017, doi: 10.1039/C7TA03334F.

[24] "Reaction Mechanism of Indium Antimonide as a Sodium Storage Material | Crystal Growth & Design." https://pubs.acs.org/doi/10.1021/acs.cgd.0c01045 (accessed Apr. 27, 2021).

[25] T. T. Tran and M. N. Obrovac, "Alloy Negative Electrodes for High Energy Density Metal-Ion Cells," *J. Electrochem. Soc.*, vol. 158, no. 12, p. A1411, Nov. 2011, doi: 10.1149/2.083112jes.

[26] V. L. Chevrier and G. Ceder, "Challenges for Na-ion Negative Electrodes," *J. Electrochem. Soc.*, vol. 158, no. 9, p. A1011, Jul. 2011, doi: 10.1149/1.3607983.